

Dysregulation of very-long-chain fatty acid metabolism causes membrane saturation and induction of the unfolded protein response

Yagmur Micoogullari^a, Sankha S. Basu^b, Jessie Ang^a, Nina Weisshaar^a, Nicholas D. Schmitt^c, Walid M. Abdelmoula^b, Begona Lopez^b, Jeffrey N. Agar^{c,d}, Nathalie Agar^b, and John Hanna^{a,*}

^aDepartment of Pathology and ^bDepartment of Neurosurgery, Harvard Medical School and Brigham and Women's Hospital, Boston, MA 02115; ^cDepartment of Chemistry and Chemical Biology and ^dDepartment of Pharmacological Sciences, Northeastern University, Boston, MA 02111

ABSTRACT The unfolded protein response (UPR) senses defects in the endoplasmic reticulum (ER) and orchestrates a complex program of adaptive cellular remodeling. Increasing evidence suggests an important relationship between lipid homeostasis and the UPR. Defects in the ER membrane induce the UPR, and the UPR in turn controls the expression of some lipid metabolic genes. Among lipid species, the very-long-chain fatty acids (VLCFAs) are relatively rare and poorly understood. Here, we show that loss of the VLCFA-coenzyme A synthetase *Fat1*, which is essential for VLCFA utilization, results in ER stress with compensatory UPR induction. Comprehensive lipidomic analyses revealed a dramatic increase in membrane saturation in the *fat1Δ* mutant, likely accounting for UPR induction. In principle, this increased membrane saturation could reflect adaptive membrane remodeling or an adverse effect of VLCFA dysfunction. We provide evidence supporting the latter, as the *fat1Δ* mutant showed defects in the function of *Ole1*, the sole fatty acyl desaturase in yeast. These results indicate that VLCFAs play essential roles in protein quality control and membrane homeostasis and suggest an unexpected requirement for VLCFAs in *Ole1* function.

Monitoring Editor
Howard Riezman
University of Geneva

Received: Jul 23, 2019
Revised: Nov 12, 2019
Accepted: Nov 13, 2019

INTRODUCTION

Misfolded proteins are toxic, and cells have developed complex stress responses to identify and eliminate them. In the unfolded protein response (UPR), misfolded proteins within the endoplasmic reticulum (ER) activate the transmembrane protein *Ire1* to carry out

This article was published online ahead of print in MBoC in Press (<http://www.molbiolcell.org/cgi/doi/10.1091/mbc.E19-07-0392>) on November 20, 2019.

Author contributions: J.H. conceived of the project. Y.M., J.A., N.W., and J.H. performed the nonlipidomic analyses. Lipidomic analyses were performed by S.S.B., Y.M., N.D.S., W.M.A., and B.L. with supervision and assistance from N.A. and J.N.A. J.H. and Y.M. wrote the manuscript with input from all of the authors.

The authors declare that they have no conflict of interest.

*Address correspondence to: John Hanna (jwhanna@bwh.harvard.edu).

Abbreviations used: ALD, adrenoleukodystrophy; CoA, coenzyme A; ER, endoplasmic reticulum; FT-ICR MS, Fourier transform-ion cyclotron resonance mass spectrometry; GFP, green fluorescent protein; HA, hemagglutinin; LESA MS, liquid-extraction surface-analysis mass spectrometry; PA, phosphatidic acid; PC, phosphatidylcholine; PE, phosphatidylethanolamine; PS, phosphatidylserine; UPR, unfolded protein response; VLCFA, very-long-chain fatty acids.

© 2020 Micoogullari et al. This article is distributed by The American Society for Cell Biology under license from the author(s). Two months after publication it is available to the public under an Attribution-Noncommercial-Share Alike 3.0 Unported Creative Commons License (<http://creativecommons.org/licenses/by-nc-sa/3.0>).

"ASCB®," "The American Society for Cell Biology®," and "Molecular Biology of the Cell®" are registered trademarks of The American Society for Cell Biology.

the unusual cytoplasmic splicing of *HAC1* mRNA (Cox and Walter, 1996). *Hac1* (Xbp1 in mammals) then coordinates the transcription of hundreds of genes that adapt the cell to ER stress (Travers et al., 2000). An exciting development in recent years has been the recognition that lipid homeostasis is critical for protein quality control. Various defects in lipid metabolism activate the UPR, and the UPR in turn stimulates the expression of lipid metabolic genes (Cox et al., 1997; Travers et al., 2000; Jonikas et al., 2009). Recent work indicates the existence of an unexpected second pathway of *Ire1* activation that operates through the membrane. In contrast to the canonical ER luminal sensing mechanism for misfolded proteins, this second pathway senses defects in the membrane ("bilayer stress") and may function independently of misfolded proteins (Promlek et al., 2011; Volmer et al., 2013; Halbleib et al., 2017). This emerging relationship between the UPR and lipid metabolism is recapitulated at the level of human disease. Obesity is a major inducer of the UPR, and weight loss reverses UPR induction (Gregor et al. 2009). Conversely, defects in the UPR pathway lead to prediabetic insulin resistance (Ozcan et al., 2004; Fu et al., 2011).

The physical and chemical properties of the membrane are critical for its many functions within the cell. These include membrane

thickness, fluidity/rigidity, and curvature, among others. These properties are largely determined by the composition of the membrane, which consists mainly of phospholipids and sterols (Harayama and Riezman, 2018; Radanovi *et al.*, 2018). The acyl groups of phospholipids can vary in both their length and degree of unsaturation, making them critical determinants of membrane biology. In response to stress, cells may attempt to maintain the appropriate physicochemical properties of the membrane by altering membrane composition. This concept, originally described in bacteria in the 1970s, has sometimes been referred to as homeoviscous adaption (Sinensky, 1971, 1974). In response to increasing temperature, for example, bacterial cells increased the proportion of saturated fatty acids in their membrane phospholipids. Similar adaptations have been observed in many other poikilothermic organisms (Ernst *et al.*, 2016), and it is thought that the general concept of altering membrane composition to preserve membrane function is applicable to all organisms, including those that regulate their own temperature.

Very-long-chain fatty acids (VLCFAs; more than 20 carbon groups) are relatively rare species, comprising only 1–2% of total fatty acids in yeast (Welch and Burlingame, 1973), and they remain poorly understood relative to other lipids. They have unique properties, including the ability to span both leaflets of the membrane bilayer, potentially stabilizing curved membranes (Kihara, 2012). Like other fatty acids, they perform multiple functions within cells: they can be used to generate ATP via beta-oxidation and to posttranslationally modify various proteins (e.g., GPI anchors), and they can serve as components of various structural and signaling lipids, mainly phospholipids and sphingolipids (Kihara, 2012). VLCFAs, like other fatty acids, may be synthesized within the cell or taken up from the environment. However, use of free fatty acids for any of these downstream processes first requires activation by thioesterification with coenzyme A (CoA). In yeast, there are five fatty acyl-CoA synthetases: Faa1–4 function primarily for long- and medium-chain fatty acids (C12–C20) while Fat1 is the major VLCFA-CoA synthetase (and shows no activity against the more abundant long-chain fatty acids) (Watkins *et al.*, 1998; Choi and Martin, 1999; Black and DiRusso 2007; Haribowo *et al.*, 2019). The critical nature of VLCFAs is underscored by the lethality of an *elo2Δelo3Δ* double mutant, those enzymes being the major VLCFA elongases (Oh *et al.*, 1997). Furthermore, inability to use VLCFAs is the direct cause of X-linked adrenoleukodystrophy (ALD), and accumulation of free VLCFAs is characteristic in these patients (Singh *et al.*, 1984; Watkins *et al.*, 2000).

Here, we sought to study the effects of VLCFA dysfunction by characterizing the *fat1Δ* mutant. We find that this mutant shows significant defects in ER protein quality control with compensatory induction of the UPR. Lipidomic analyses indicated a dramatic increase in membrane saturation in this mutant involving the two most abundant phospholipid species in the cell. In principle, this increase in membrane saturation could reflect an adaptive response to defects in the *fat1Δ* mutant or an adverse effect related to loss of Fat1. Our data support the latter, as loss of Fat1 compromised the function of Ole1, the sole fatty acid desaturase in yeast. These results indicate a critical role for VLCFAs in protein quality control and membrane homeostasis and suggest an unexpected link between VLCFAs and stearyl-CoA desaturases.

RESULTS

Fat1 functions in ER protein quality control

Increasing evidence suggests a close relationship between lipid homeostasis and protein quality control. To characterize the role of VLCFAs in protein quality control, we knocked out *FAT1*, the major very-long-chain fatty acyl-CoA synthetase in yeast. We started by

measuring phenotypic sensitivity to the amino acid analogue canavanine, a widely used inducer of proteotoxic stress. Canavanine is incorporated into newly synthesized proteins in place of arginine, causing them to misfold. The *fat1Δ* mutant showed significantly reduced growth when challenged with canavanine (Figure 1A and Supplemental Figure S1), and this growth defect was fully complemented by restoration of Fat1 expression via a low-copy centromeric plasmid bearing the endogenous *FAT1* promoter (Supplemental Figure S2). Null mutants of two long-chain fatty acyl-CoA synthetases, *Faa1* and *Faa4*, did not show sensitivity to canavanine (Figure 1A).

Canavanine is expected to cause protein misfolding throughout the cell. To determine whether Fat1 might have a more compartment-specific function, we used tunicamycin, an inhibitor of ER glycosylation that induces protein misfolding and subsequent ER stress. The *fat1Δ* mutant showed a significant growth defect upon exposure to tunicamycin (Figure 1B). This tunicamycin sensitivity suggested a role for Fat1 in ER homeostasis, defects in which are compensated by the UPR. To determine whether the *fat1Δ* mutant triggered the UPR, we used a UPR reporter that consists of four copies of the *HAC1* binding site (“UPRE”) fused to green fluorescent protein (GFP) (Figure 1C). We detected an ~60% increase in fluorescence in the *fat1Δ* mutant, even in the absence of an exogenous proteotoxic stress, consistent with tonic up-regulation of the UPR in this mutant (Figure 1D). This observation raised the possibility that constitutive activation of the UPR might compensate for detrimental effects of the *fat1Δ* mutant. To test this hypothesis, we constructed a *fat1Δhac1Δ* double mutant and tested its sensitivity to the divalent metal cadmium chloride, which is known to induce ER stress (Gardarin *et al.*, 2010). Loss of Hac1 strongly sensitized the *fat1Δ* mutant to cadmium toxicity (Figure 1E). A similar synthetic effect was observed with tunicamycin (unpublished data). Together, these data indicate a novel role for Fat1 in ER homeostasis, with loss of Fat1 being compensated by constitutive UPR induction. This conclusion is further supported by a prior yeast genome-wide survey that identified *fat1Δ* among mutants showing constitutive UPR induction (Jonikas *et al.*, 2009).

Prior work indicates that the UPR controls the expression of multiple genes involved in lipid metabolism (Travers *et al.*, 2000). We therefore sought to determine whether Fat1 might be a target of the UPR. We induced the UPR using tunicamycin, which resulted in strong splicing of *HAC1* (Supplemental Figure S3). By contrast, there was no induction of *FAT1* (Supplemental Figure S3). Thus, Fat1 regulates the UPR but is not itself a UPR target.

Fat1 is a key mediator of membrane homeostasis

We sought to determine which aspect of VLCFA function might explain the role of Fat1 in ER stress. Given the increasingly appreciated role of membrane homeostasis in proper ER function, we decided to take a mass spectrometry-based lipidomics approach to this question. We cultured wild-type and *fat1Δ* cells and extracted total cellular lipids using a standard methanol/chloroform-based protocol (Knittelfelder and Kohlwein, 2017). We then analyzed these lipids using Fourier transform-ion cyclotron resonance mass spectrometry (FT-ICR MS) (Ghaste *et al.*, 2016). This technique allows for highly precise mass measurements (<1 ppm) and as such facilitates the assignment of individual spectral peaks with high confidence.

As an internal control, we first examined the relative abundance of free VLCFAs, which are known to accumulate in the *fat1Δ* mutant owing to its inability to activate them for downstream functions (Watkins *et al.*, 1998; Choi and Martin, 1999). As shown in Figure 2A, the levels of the long-chain fatty acids palmitic (C16:0) and stearic

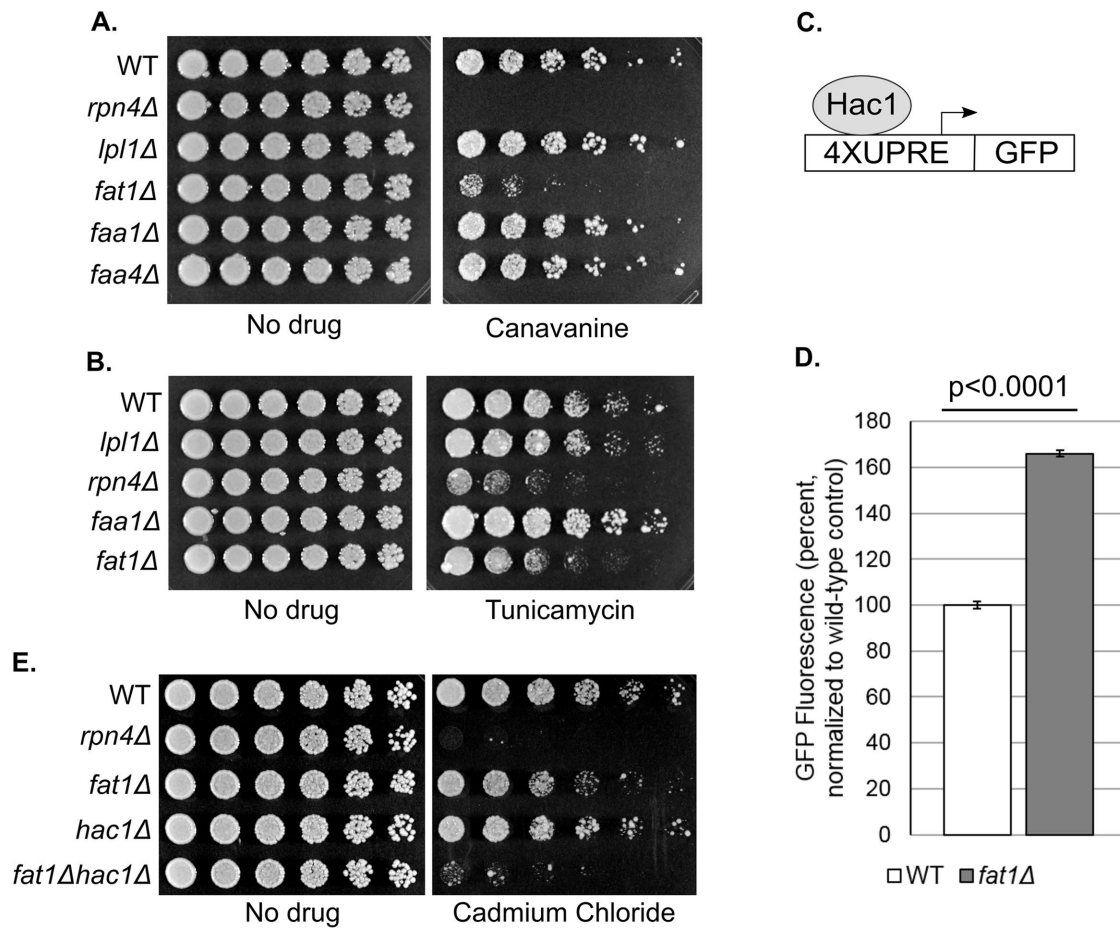


FIGURE 1: VLCFA dysfunction leads to ER stress and compensatory induction of the UPR. (A) Growth of the indicated strains in the presence or absence of the amino acid analogue canavanine (2.5 $\mu\text{g/ml}$). Cells were spotted in threefold serial dilutions and cultured at 30°C for 2 d. (B) Growth of the indicated strains in the presence or absence of tunicamycin (2.5 $\mu\text{g/ml}$), an inducer of ER stress. Cells were spotted in threefold serial dilutions and cultured at 30°C for 2 d. (C) Schematic of the UPR reporter. Four copies of the Hac1 recognition sequence (UPRE) were fused to the coding region of GFP and integrated into the genome. (D) Constitutive induction of the UPR in the *fat1* Δ mutant. Results represent the mean GFP signal from four technical replicates and are normalized to the wild-type (WT) control. Error bars represent SDs. Results were also significant by two-tailed Student's *t* test ($p < 0.0001$). (E) Abrogation of UPR induction by Hac1 sensitizes *fat1* Δ cells to ER stress. The indicated strains were cultured in the presence or absence of cadmium chloride (60 μM), a known inducer of the UPR (Gardarin *et al.*, 2010). Cells were spotted in threefold serial dilutions and cultured at 30°C for 2–3 d.

acid (C18:0) were comparable between wild type and *fat1* Δ . By contrast, there was a marked accumulation of 22-, 24-, and 26-carbon free fatty acids (Figure 2A; see Supplemental Table S2 for full lipidomic profiles). This inability to use VLCFAs would be expected to decrease the abundance of lipid species that contain VLCFAs. Indeed, we found that the levels of phytosphingosine, which is modified by a VLCFA to generate phytoceramide, were increased in the *fat1* Δ mutant, while the abundance of three VLCFA-containing ceramides was decreased (Figure 2B).

Phospholipids are the major constituents of membranes. The various properties of phospholipids have a major impact on the physical and chemical properties of membranes. These variables include the relative abundance of different phospholipids with their different head groups, the length of their fatty acyl chains, and the degree of unsaturation of their fatty acyl chains. In yeast, phosphatidylcholine (PC) and phosphatidylethanolamine (PE) are the most abundant, constituting ~75% of total cellular phospholipids and ~60% of ER phospholipids (Klug and Daum, 2014). Unsaturated

phospholipids predominate in yeast, with ~70% or more of phospholipids harboring a double bond in each fatty acyl group.

A surprising and dramatic finding from the lipidomic analysis was that the two most abundant PC species in the cell showed a striking increase in saturation in the *fat1* Δ mutant (Figure 2, C and D, and Supplemental Figure S4). These were the 32-carbon PC (typically two 16-carbon fatty acyl groups) and 34-carbon PC (typically one 16- and one 18-carbon fatty acyl group). In wild-type cells, the fully unsaturated forms (32:2 or 34:2) predominated over the monounsaturated forms (32:1 or 34:1) (Figure 2, C and D, and Supplemental Figure S4). Note that the fully saturated species (32:0 or 34:0) were much less abundant and are not visible above the background peaks in Figure 2C (Supplemental Table S2 and Supplemental Figure S5). In the *fat1* Δ mutant, by contrast, the relative abundance of di-unsaturated species was decreased with a concomitant increase in the respective monounsaturated species (Figure 2, C and D) and the fully saturated species to a lesser extent (Supplemental Figure S5). This increase in overall membrane saturation was of

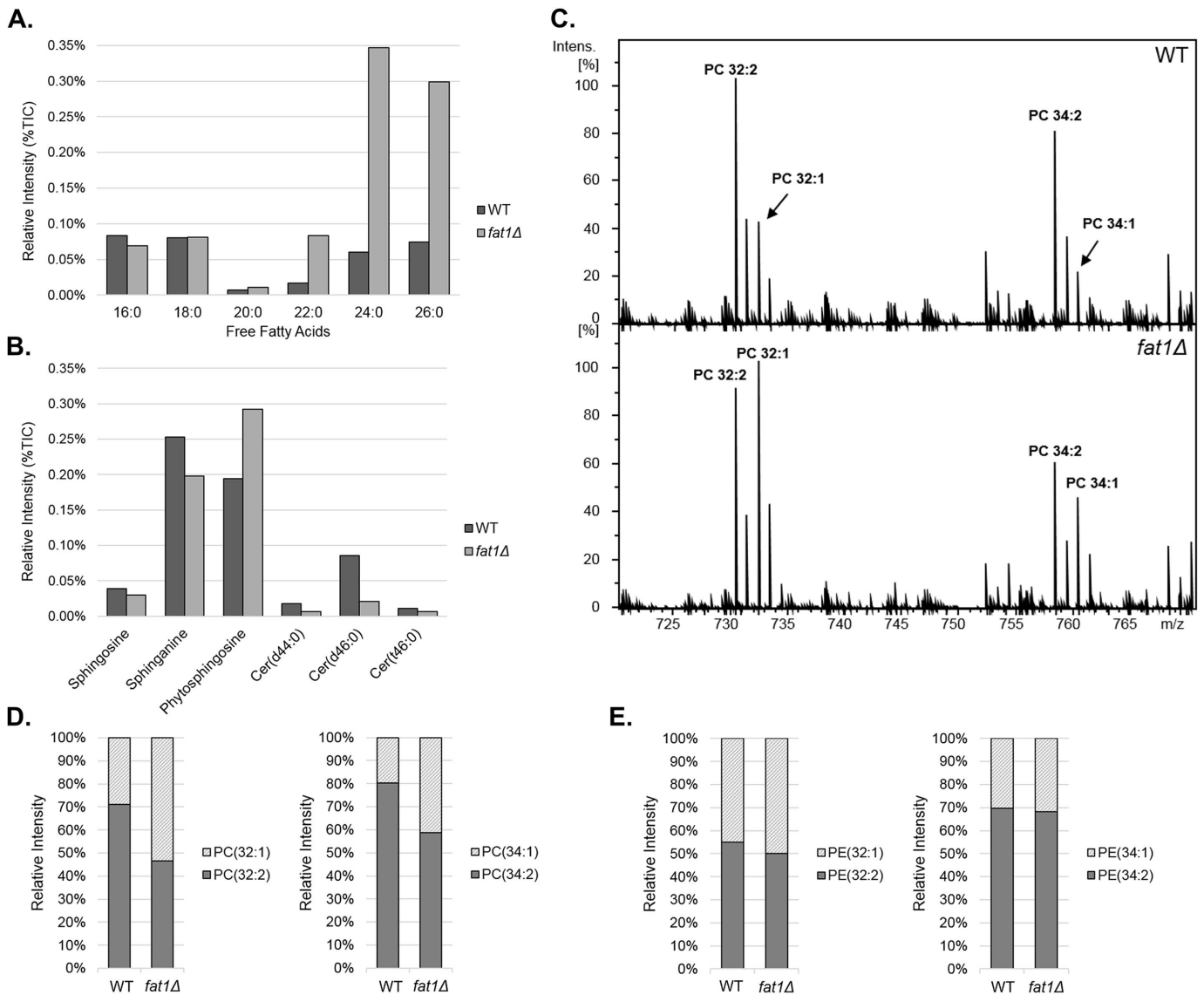


FIGURE 2: Increased phospholipid saturation in the *fat1Δ* mutant. (A) Relative intensity of long (C16–C20) and very-long-chain (C22–C26) fatty acids in the wild type (WT) and *fat1Δ* mutant, as determined by comprehensive FT-ICR MS-based lipidomics. Relative intensity is expressed as a percentage of the total ion current (TIC). Similar results were obtained in more than three independent experiments. The mass to charge ratios are 291.2095 (16:0), 319.2408 (18:0), 347.2721 (20:0), 375.3033 (22:0), 403.3346 (24:0), and 431.3658 (26:0). (B) Relative intensity of selected lipid species in the wild type and *fat1Δ* mutant. The three ceramide (Cer) species shown contain a VLCFA moiety, whereas sphingosine, sphinganine, and phytosphingosine are precursors for ceramide synthesis. Relative intensity is expressed as a percentage of the TIC. Similar results were obtained in more than three independent experiments. The mass to charge ratios are 300.2891 (sphingosine), 302.3047 (sphinganine), 318.2995 (phytosphingosine), 680.6764 (Cer (d44:0)), 708.7663 (Cer(d46:0)), and 724.7021 (Cer(t46:0)). (C) Raw positive ion mode spectra from lipidomic profiles of wild-type and *fat1Δ* cells. The relative intensity of the two most abundant phosphatidylcholine species in yeast (PC-32 and PC-34) are indicated. PC (32:2) and PC (34:2) represent the di-unsaturated forms; PC (32:1) and PC (34:1) represent the monounsaturated forms. Relative intensity is expressed as peak intensity normalized to the base peak of the displayed *m/z* window. Similar results were obtained in more than 15 independent experiments (see also Figure 4, C and D). The mass to charge ratios are 730.5381 (32:2), 732.5538 (32:1), 758.5694 (34:2), and 760.5809 (34:1). (D) Relative intensity of di-unsaturated and monounsaturated PC-32 (left) and PC-34 (right) species in the wild type and *fat1Δ* mutant. The fraction of each species as a total of the sum of the two species is plotted. Similar results were obtained in more than 15 independent experiments. (E) Relative intensity of di-unsaturated and monounsaturated PE-32 (left) and PE-34 (right) species in the wild type and *fat1Δ* mutant. The fraction of each species as a total of the sum of the two species is plotted. Similar results were obtained in more than 10 independent experiments.

interest because increased membrane saturation is known to be a potent trigger of the UPR in both yeast and higher organisms (Pineau *et al.*, 2009; Volmer *et al.*, 2013).

Interestingly, the *fat1Δ*-dependent increase in saturation was much more pronounced for PC than for the other major phospholipid species. The PC precursors phosphatidic acid (PA), PE, and

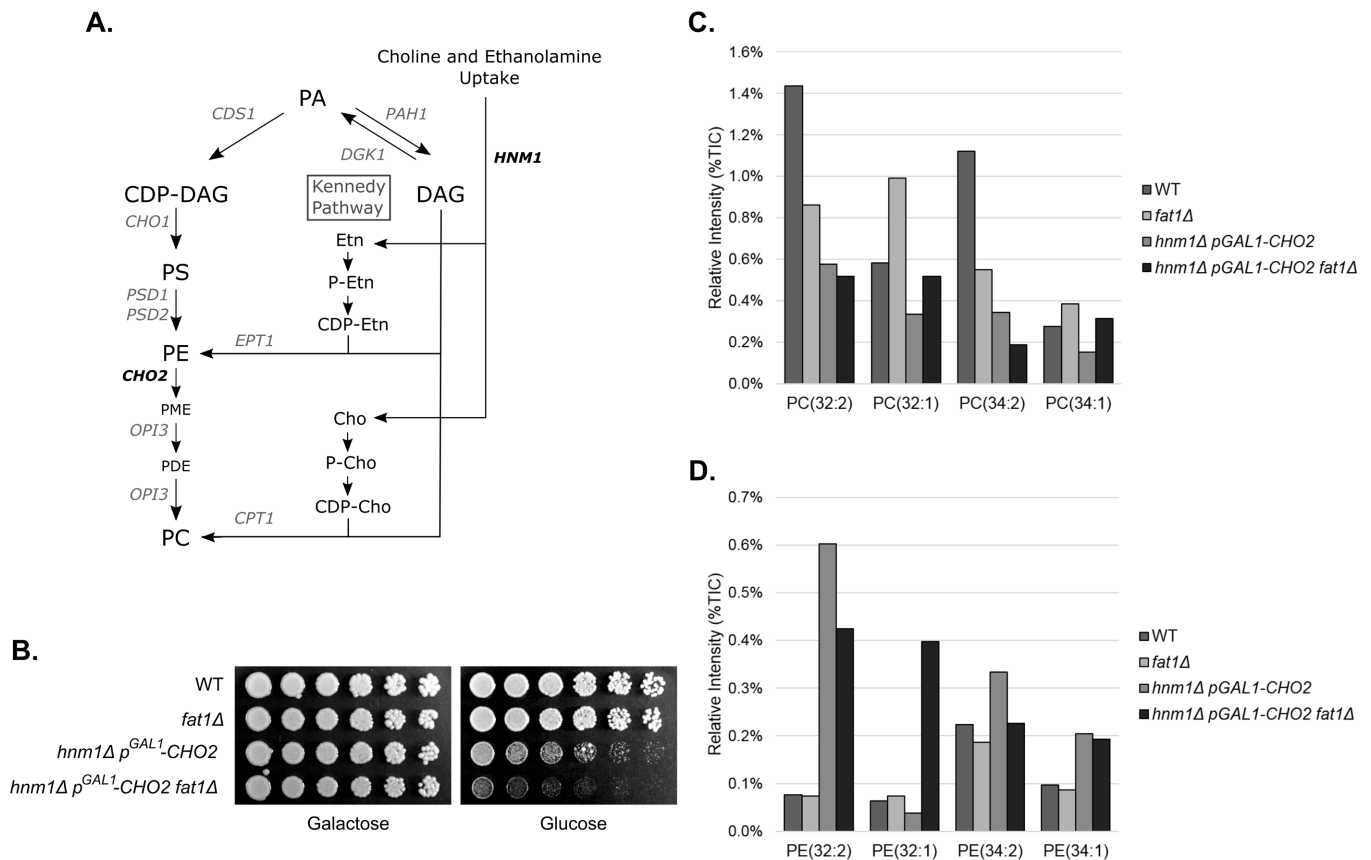


FIGURE 3: Loss of Fat1 stimulates phosphatidylethanolamine saturation upon inhibition of phosphatidylcholine synthesis. (A) Schematic of PC synthesis in yeast. See Carman and Han (2009) for further details. PA, phosphatidic acid; DAG, diacylglycerol; Etn, ethanolamine; P-Etn, phosphoethanolamine; CDP-Etn, cytidine diphosphate-ethanolamine; Cho, choline; P-Cho, phosphocholine; CDP-Cho, cytidine diphosphate-choline; CDP-DAG, cytidine diphosphate-diacylglycerol; PS, phosphatidylserine; PE, phosphatidylethanolamine; PME, phosphatidylmonomethylethanolamine; PDE, phosphatidyl dimethylethanolamine; PC, phosphatidylcholine, WT, wild type. (B) Synthetic growth defect of the *fat1*Δ mutation with *p*^{GAL1}-*CHO2 hnm1*Δ. Cells were spotted in threefold serial dilutions onto plates containing galactose ("Cho2 on") or glucose ("Cho2 off") and cultured at 30°C for 2 d. (C) Relative intensity of the indicated PC species in the indicated strains, expressed as percentages of the TIC. All strains were cultured in glucose-containing media for 36 h to repress Cho2 expression. Similar results were obtained in three independent experiments. (D) Relative intensity of the indicated PE species in the indicated strains, expressed as percentages of the TIC. All strains were cultured in glucose-containing media for 36 h to repress Cho2 expression. Similar results were obtained in three independent experiments.

phosphatidylserine (PS) also showed some evidence of increased saturation in the *fat1*Δ mutant (Supplemental Figure S6). This was a modest increase for PA, and a very mild increase for PE and PS; in all cases, the effect was mainly seen with the 32-carbon species (Figure 2E and Supplemental Figure S6). Phosphatidylinositol, in contrast, existed mainly as the monounsaturated species (i.e., 32:1 and 34:1) and did not show evidence of increased saturation in the *fat1*Δ mutant (Supplemental Figure S6).

To determine whether flux within pathways of phospholipid synthesis could impact Fat1-dependent membrane saturation, we impaired the two major pathways of PC synthesis by knocking out Hnm1 (which imports extracellular choline and ethanolamine for PE/PC synthesis by the Kennedy pathway) and by knocking down Cho2 (which mediates the de novo CDP-DAG synthesis pathway) by placing Cho2 expression under the control of the inducible *GAL1* promoter (Figure 3A). Under repressing conditions, this mutant results in a relative accumulation of PE over PC and strongly induces the UPR (unpublished data; see also Thibault *et al.*, 2012; Vevea

et al., 2015). Interestingly, elimination of Fat1 in this *p*^{GAL1}-*CHO2 hnm1*Δ mutant further impaired growth, even in the absence of stress (Figure 3B). We analyzed total cellular lipids in this genetic background. Loss of Fat1 again resulted in increased saturation of the 32- and 34-carbon PC species (Figure 3C). In comparison to the wild-type background, loss of Fat1 in the *p*^{GAL1}-*CHO2 hnm1*Δ mutant now resulted in much larger increases in PE saturation, particularly for the 32-carbon species (Figure 3D). These findings suggest that multiple phospholipid species are subject to increased saturation upon loss of Fat1, and these effects may be responsive to changes in flux within pathways of phospholipid synthesis.

Mechanism of increased membrane saturation in the *fat1*Δ mutant

In principle, there are two potential explanations for the increase in membrane saturation in the *fat1*Δ mutant (Figure 4A). The first is that one or more acyltransferases may alter membrane saturation by preferentially transferring saturated fatty acyl groups to

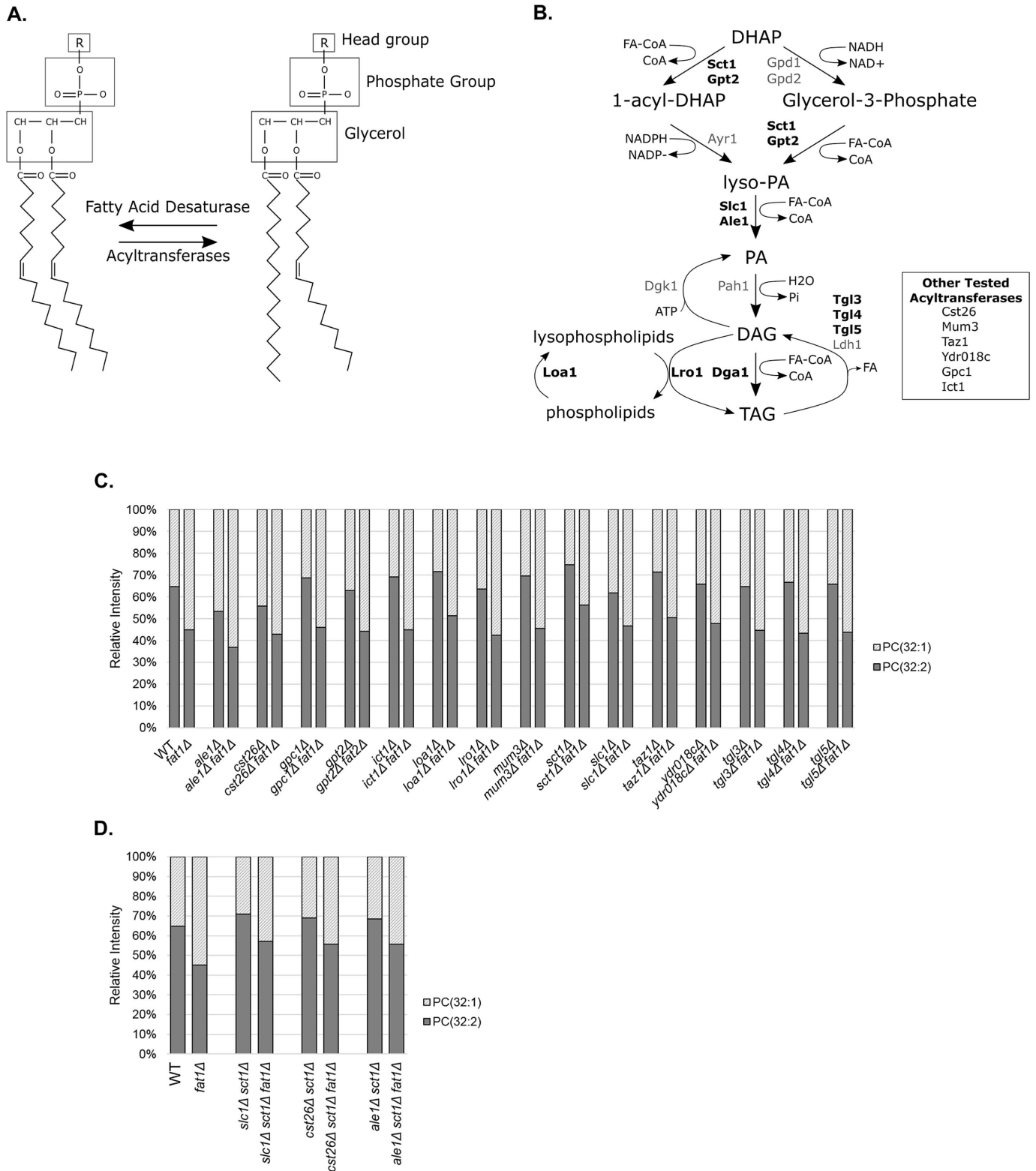
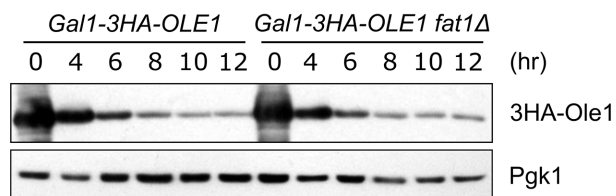


FIGURE 4: Persistence of *fat1Δ*-induced PC saturation in diverse acyltransferase mutants. (A) Schematic diagram of phospholipid saturation. Increased fatty acid saturation could result from the increased activity of an acyltransferase that preferred saturated fatty acids or from decreased activity of the sole fatty acyl desaturase in yeast, *Ole1*. (B) Schematic diagram highlighting the role of selected acyltransferases and potential acyltransferases in lipid metabolism. DHAP, dihydroxyacetone phosphate; PA, phosphatidic acid; lyso-PA, 1-acyl-glycerol-3-phosphate; DAG, diacylglycerol; TAG, triacylglycerol; FA, fatty acid; FA-CoA, fatty acyl-CoA. (C, D) Relative intensity of PC (32:2 and 32:1) in the indicated strains. The fraction of each species as a total of the sum of the two species is plotted. Similar results were obtained in at least two independent experiments. Many of the mutant pairs were analyzed in more than four independent experiments. These experiments were performed using LESA MS.

A.



B.

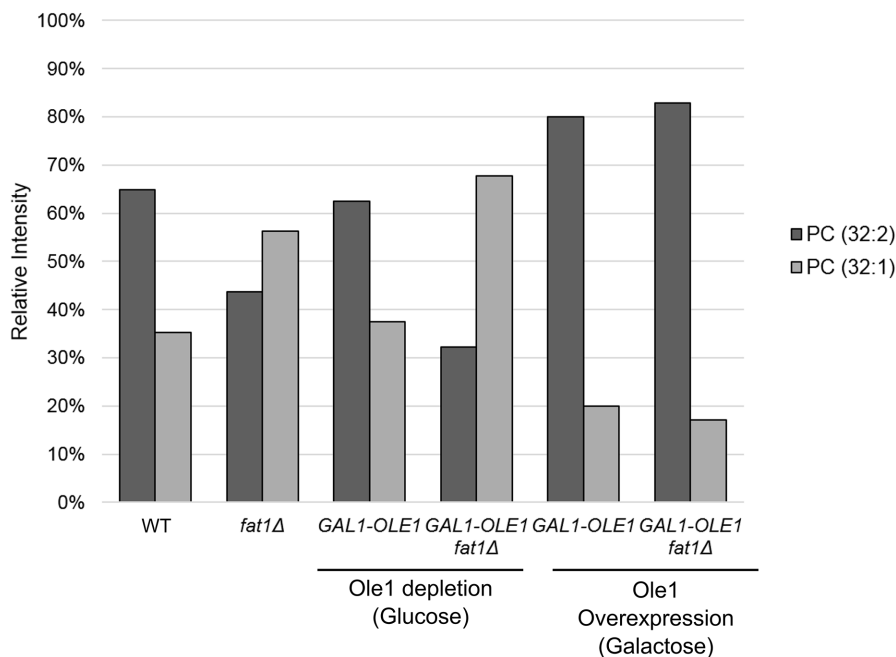


FIGURE 5: Modulation of *fat1Δ*-induced phospholipid saturation by the desaturase Ole1. (A) Ole1 protein levels after *GAL1*-promoter shutoff. Whole-cell extracts were prepared at the indicated time points and analyzed by SDS-PAGE followed by immunoblotting. Top, anti-HA antibody; bottom, anti-Pgk1 antibody (loading control). (B) Relative intensities of PC (32:1 and 32:2) species in the indicated strains. For Ole1 knockdown, cells were cultured in glucose-containing media for 8 h (see A). Culturing in galactose-containing media actually resulted in Ole1 overexpression, as can be seen in the increased unsaturation seen in the *GAL1-Ole1* strain vs. the wild-type strain (compare first and fifth samples). Relative intensity is expressed as a percentage of the combined intensities of the two molecules. Similar results were obtained in three independent experiments. These experiments were performed using LESA MS.

phospholipids. This could occur during new phospholipid synthesis or through remodeling of existing membrane phospholipids by replacing unsaturated acyl groups with saturated acyl groups. The second major possibility would be a decrease in the function of the sole desaturating enzyme in yeast, Ole1.

There are at least 23 known or predicted acyltransferases in yeast involved in various aspects of lipid metabolism (Figure 4B). A key intermediate in the de novo generation of PC is PA. Acylation at PA's sn-1 position is carried out by the partially redundant enzymes Sct1 and Gpt2, while acylation at its sn-2 position is carried out by Slc1 and Ale1. These enzymes were thus prime candidates for a potential remodeling function. Indeed, Sct1 was previously reported to prefer saturated fatty acids and to antagonize the function of Ole1 (DeSmet *et al.*, 2012). We knocked out each acyltransferase in the *fat1Δ* background and compared the degree of saturation with that of the parental strain. Any double mutant showing a failure to increase the degree of PC saturation would be considered as a prime candidate for mediating this *fat1Δ*-dependent change. We tested 15 acyltrans-

ferase mutants: all of them retained a strong increase in PC saturation when Fat1 was deleted (Figure 4C). A challenge in studying these enzymes is the significant degree of functional redundancy within the family. Cells will not tolerate a complete loss of sn-1 (i.e., *sct1Δgpt2Δ*) or sn-2 activity (i.e., *slc1Δale1Δ*), but will tolerate combined loss of one sn-1 and one sn-2 acyltransferase. Therefore, we constructed *sct1Δslc1Δ* and *sct1Δale1Δ* double mutants and combined them with the *fat1Δ* mutation. However, the *fat1Δ*-dependent increase in saturation persisted (Figure 4D). Despite considerable efforts, we have no evidence at present to support a role for an acyltransferase in this novel *fat1Δ*-dependent membrane saturation effect, although it should be noted that the functional redundancy within this enzyme class, combined with synthetic lethality of certain mutant combinations, makes it difficult to definitively exclude this possibility.

The second major potential explanation for increased membrane saturation in the *fat1Δ* mutant would be a reduction in desaturation by Ole1 (Figure 4A). *Ole1* is an essential gene, so we opted to place its expression under the control of the *GAL1* promoter, which is operational in the presence of galactose and repressed in the presence of glucose. We also included an N-terminal 3xHA (hemagglutinin) tag to allow for detection by immunoblot. During promoter shutoff, there is a time window after which Ole1 protein levels have been reduced but before cells begin to lose viability. At 8 h after promoter shutoff, cells retained full viability but showed a significant, although not complete, reduction in Ole1 levels (Figure 5A). We extracted lipids and determined the full lipidomic profiles as before. In *fat1Δ* cells depleted of Ole1, the extent of PC saturation was substantially increased compared with the *fat1Δ* mutant

alone (Figure 5B, compare second and fourth samples). Interestingly, in the wild-type background, PC saturation was largely preserved upon Ole1 knockdown (Figure 5B, compare first and third samples). This suggests that the residual Ole1 protein remaining after promoter shutoff (Figure 5A) is sufficient to maintain normal membrane saturation in wild-type cells but not in the *fat1Δ* mutant.

The *p^{GAL1}-OLE1* strain also allowed us to determine the effect of Ole1 overexpression on this process. This is due to the strength of the *GAL1* promoter: Ole1 is actually overexpressed when cultured in galactose compared with endogenous expression, and this can be readily seen in the increased relative abundance of di-unsaturated PC (32:2) in galactose media (Figure 5B, compare first and fifth samples). Remarkably, Ole1 overexpression resulted in a complete abrogation of the *fat1Δ*-dependent increase in PC saturation (Figure 5B).

Evidence that Ole1 function may depend on Fat1

The preceding results suggest that a reduction in Ole1 function may contribute to the *fat1Δ*-dependent increase in membrane

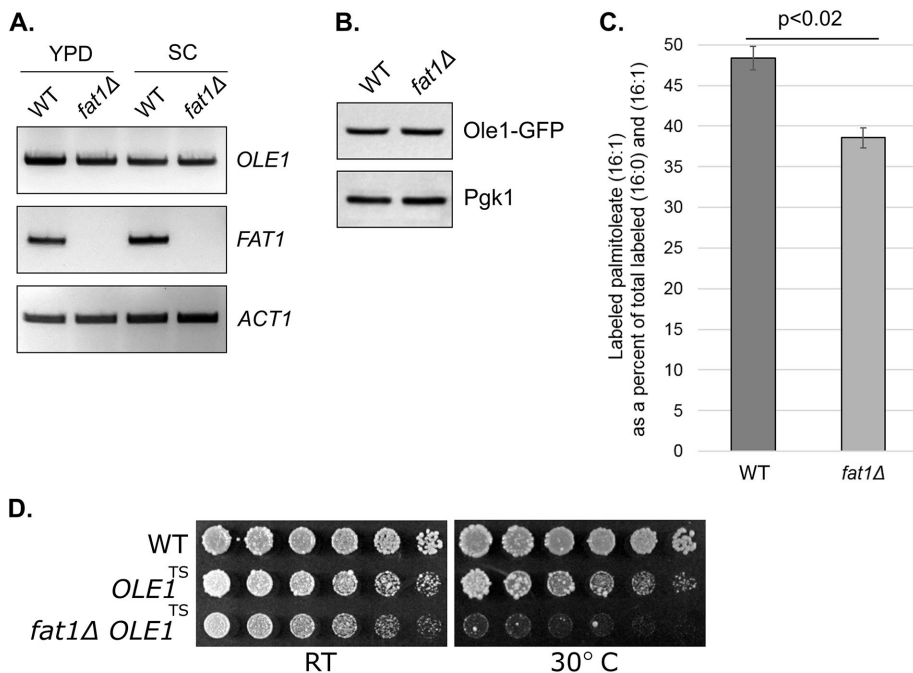


FIGURE 6: Ole1 function is dependent on Fat1. (A) *OLE1* mRNA levels, as determined by RT-PCR, in wild-type (WT) and *fat1Δ* strains grown in rich (YPD) or synthetic complete (SC) media. Middle, *FAT1* mRNA levels; bottom, *ACT1* mRNA levels (loading control). (B) Ole1 protein levels in the wild type and *fat1Δ* mutant. Whole-cell extracts were prepared at steady state from exponentially growing cultures and analyzed by SDS-PAGE followed by immunoblotting. An integrated Ole1-GFP strain was used to allow for immunohistochemical detection (top, anti-GFP antibody). Bottom, anti-Pgk1 antibody (loading control). (C) Generation of ¹³C-labeled palmitoleic acid (16:1) from ¹³C-labeled palmitic acid (16:0) in wild-type and *fat1Δ* cells. Cells were cultured with labeled palmitic acid at 50 μM for 7 h. Total lipids were extracted, and the abundance of ¹³C-labeled palmitoleic acid was determined by FT-ICR MS. Relative abundance of ¹³C-labeled palmitoleic acid is shown as a percent of the total labeled (16:0) and (16:1) fatty acid detected. Error bars represent SDs from two independent experiments. Results were also significant by two-tailed Student's *t* test ($p < 0.02$). (D) Loss of Fat1 strongly compromises growth of a temperature-sensitive *Ole1* mutant. Cells were spotted in threefold serial dilutions and cultured at 24°C ("RT") and 30°C for 2–4 d.

saturation. In principle, this could be due to a decrease in abundance or activity of Ole1 (or both) in the *fat1Δ* mutant. Loss of the Cdc48 cofactor Ubx2, for example, causes increased membrane saturation via decreased *OLE1* transcription (Surma *et al.*, 2013). In contrast, we saw no difference in Ole1 abundance at either the mRNA level (Figure 6A) or the protein level (Figure 6B) in the *fat1Δ* mutant. We next monitored Ole1 localization using a C-terminally tagged Ole1-GFP expressed from the endogenous locus. In wild-type cells, Ole1 showed both perinuclear ER localization and more cortical staining, consistent with prior studies (Supplemental Figure S7; Tatzert *et al.*, 2002). A similar pattern of Ole1 localization was seen in the *fat1Δ* mutant (Supplemental Figure S7).

To measure Ole1 activity, we used ¹³C-labeled palmitic acid (16:0). Because Ole1 is the sole desaturase in yeast, generation of labeled 16:1 palmitoleic acid should reflect Ole1 activity. Saturated fatty acid supplementation is toxic at high concentrations. Therefore, we used a low concentration of labeled palmitic acid (50 μM) and verified that there was no effect on cellular growth. ¹³C-labeled palmitoleic acid (16:1) levels were significantly decreased in the *fat1Δ* mutant, consistent with decreased Ole1 function in this mutant (Figure 6C).

The preceding data suggest that Ole1 function is partially dependent on Fat1. This model predicts that loss of Fat1 should be

deleterious in an Ole1 hypomorphic mutant. We therefore knocked out Fat1 in a temperature-sensitive mutant of Ole1 (Tatzert *et al.*, 2002). In wild-type cells, loss of Fat1 had no effect on growth under normal conditions (Figure 1, A, B, and E). In contrast, loss of Fat1 strongly compromised growth in the *ole1^{ts}* mutant, even in the absence of stress (Figure 6D).

DISCUSSION

Recent work suggests an important and unexpected relationship between the UPR and lipid metabolism. The UPR responds not just to misfolded proteins within the ER lumen, but to the state of the ER membrane. This so-called bilayer stress is sensed directly by Ire's transmembrane domain (Promlek *et al.*, 2011; Volmer *et al.*, 2013; Halbleib *et al.*, 2017). Lipid defects known to trigger the UPR include increased phospholipid saturation, defects in PC synthesis, inositol depletion, and increased sterol accumulation (Pineau *et al.*, 2009; Ariyama *et al.*, 2010; Thibault *et al.*, 2012; Vollmer *et al.*, 2013; Vevea *et al.*, 2015). Why the UPR has evolved to sense membrane aberrancies remains somewhat uncertain. One possibility is that altered membrane compositions may ultimately trigger protein misfolding in the ER such that early sensing of membrane defects could provide an anticipatory or pre-emptive response (Pineau *et al.*, 2009; Rutkowski and Hegde, 2010). Alternatively, the UPR's ability to sense membrane defects could represent an adaptive program that is separate from and independent of protein misfolding.

VLCFAs are relatively rare, comprising only 1–2% of total fatty acids in yeast (Welch and Burlingame, 1973), and remain poorly understood relative to other lipid species. Here, we identify two novel cellular roles for VLCFAs: they protect against ER stress and are required for membrane homeostasis. These functions appear to be tightly linked, as the dramatic increase in overall membrane saturation in the *fat1Δ* mutant provides a potentially compelling explanation for the constitutive UPR induction in this mutant. Increased membrane saturation is a known inducer of the UPR from yeast to humans and may be triggered by multiple routes, including addition of exogenous saturated fatty acids, direct knockdown of desaturase function, perturbation of heme synthesis (which is essential for desaturase function), and others (Pineau *et al.*, 2009; Ariyama *et al.*, 2010; Volmer *et al.*, 2013; Hou *et al.*, 2014). It is worth noting that a prior study independently identified negative synthetic genetic relationships between Fat1 and the UPR (via both Hac1 and Ire1) and between Fat1 and PC synthesis (via both Cho2 and Opi3) (Surma *et al.*, 2013), further supporting these surprising relationships between Fat1, the UPR, and phospholipid metabolism.

The mechanism of increased membrane saturation in the *fat1Δ* mutant was also unexpected. We initially wondered whether it might reflect an adaptive response to defective VLCFA use, similar to the previously described concept of homeoviscous adaptation, whereby cells attempt to maintain critical membrane

functions/properties under stress by altering membrane composition (Sinensky, 1971, 1974; Ernst *et al.*, 2016). We tested the possibility that an acyltransferase with a preference for saturated fatty acids could achieve this sort of membrane remodeling, but found no evidence to support this model. Rather, we found evidence that the function of Ole1, the sole desaturase in yeast, was compromised in the *fat1Δ* mutant. Several lines of investigation support this notion. First, overexpression of Ole1 suppressed *fat1Δ*-induced PC saturation, while knockdown of Ole1 exacerbated it (Figure 5B). Second, desaturation of a labeled exogenously added 16:0 fatty acid, which in principle should be entirely dependent on Ole1, was decreased in the *fat1Δ* mutant (Figure 6C). Third, loss of Fat1 in an *ole1^{ts}* mutant has a synthetic negative effect, indicating that Fat1 positively regulates Ole1's function in vivo (Figure 6D).

This apparent relationship between Ole1 and VLCFA metabolism is, to our knowledge, novel, and raises key questions as to its mechanism. Owing to its inability to activate VLCFAs, the *fat1Δ* mutant has at least two major defects: 1) it is deficient in synthesizing complex lipid species that contain VLCFAs, and 2) it accumulates high levels of free VLCFAs. At present, we do not know whether Ole1 dysfunction is caused by a toxic accumulation of VLCFAs or a deficiency of a critical VLCFA-containing species. Distinction between these models has been hampered by the high insolubility of VLCFAs, which makes adding exogenous VLCFAs to cells challenging. We determined the lipidomic profiles of the *elo2Δ* and *elo3Δ* single mutants, which are each deficient in the synthesis of VLCFAs: neither showed an increase in PC saturation (unpublished observations). Similarly, a mutant of the ceramide synthase complex, *lac1Δ*, also failed to show an increase in PC saturation (unpublished observations). These findings point to the specificity of the *fat1Δ* mutant in regulating membrane saturation. Ostensibly, these findings could argue that a toxic accumulation of VLCFAs drives the described features of the *fat1Δ* mutant. However, this interpretation is complicated by partial redundancy between Elo2 and Elo3 and between Lac1 and other members of the ceramide synthase complex. Thus, it remains possible that optimal function of Ole1, which is itself an ER membrane protein, requires a membrane milieu that contains VLCFAs.

This work has focused mainly on phospholipids, but it is likely that Fat1 has important effects on other lipid classes. Ceramides are particularly relevant, as many ceramides incorporate VLCFAs. Indeed, our data indicate accumulation of the direct ceramide precursor phytosphingosine, as well as decreased relative abundance of three defined VLCFA-containing ceramide species (Figure 2B). These data confirm that ceramide synthesis is compromised in the *fat1Δ* mutant. However, ceramides in general were poorly represented in our lipidomic analysis (Supplemental Table S2). This is likely due to the fact that our lipid extraction method is optimized for the detection of phospholipids and that phospholipids are much more abundant than ceramides. Lipidomic analyses using extraction methods optimized for ceramides thus represent an important area of future study for Fat1.

A number of human diseases are caused by defects in VLCFA metabolism. X-linked ALD is a fatal neurodegenerative disorder caused by loss-of-function mutations in ABCD1, which mediates import of VLCFAs into the peroxisome for beta-oxidation (Wiesinger *et al.*, 2015). Similar to the *fat1Δ* mutant, ALD is characterized by the accumulation of VLCFAs in both plasma and tissues, and this is thought to be a major contributor to the disease phenotype. Alternatively, mutations in two different VLCFA elongases (ELOVL4 and ELOVL5) each lead to spinocerebellar ataxia, while mutation of ELOVL1 causes a disorder characterized by hypomyelination, facial dysmorphism, and ichthyosis (Kutkowska-Kaźmierczak *et al.*, 2018;

Mueller *et al.*, 2019). It will be important to determine whether defects in membrane homeostasis and protein quality control, as seen in the *fat1Δ* mutant, have relevance for these and other diseases of VLCFA metabolism.

MATERIALS AND METHODS

Strains and plasmids

Yeast strains and plasmids are listed in Supplemental Table S1. Yeast strains are isogenic with BY4741 unless otherwise specified. Standard PCR-based methods were used for yeast gene deletions and epitope tagging. YPD medium consisted of 1% yeast extract, 2% Bacto peptone, and 2% dextrose. YPGal medium consisted of 1% yeast extract, 2% Bacto peptone, and 2% galactose. Synthetic medium consisted of 0.7% Difco yeast nitrogen base supplemented with adenine, uridine, amino acids, and 2% dextrose. Plasmid selection was by omission of the appropriate amino acid or uridine from synthetic medium.

Flow cytometry

Logarithmic-phase cultures grown in synthetic medium were incubated for 10 min with 1 μg/ml propidium iodide to allow for identification of dead cells. We analyzed 15,000 cells from each sample, using a MACSQuant Analyzer 10 (Miltenyi Biotec). Data analysis was performed with FlowJo software (Ashland, OR). Dead cells were eliminated from the analysis using red fluorescence intensity, and medium-sized cells were selected for further analysis. Median GFP values were calculated for each sample after subtraction of background signal. Average signal intensities of quadruplicates were plotted with SD.

Immunoblotting

Whole-cell extracts of logarithmic-phase cultures were prepared by a lithium acetate/sodium hydroxide method as previously described (Weisshaar *et al.*, 2017). Extracts were analyzed by standard SDS-PAGE followed by immunoblotting. The following antibodies were used: anti-HA-peroxidase (12013819001; Roche), anti-Pgk1 (459250; Invitrogen), and anti-GFP (11814460001; Roche).

Lipid extraction

Total yeast lipid extracts were prepared as previously described (Knittelfelder and Kohlwein, 2017). Overnight cultures grown at 30°C in rich media ($OD_{600} \sim 5$) were diluted into fresh media (starting $OD_{600} = 0.1$) and cultured for 6 h to a final OD_{600} of ~ 0.8 . These logarithmic-phase cells were washed with water and resuspended in cold $CHCl_3/MeOH$ (2:1) solution. Cells were disrupted with glass beads at 3200 rpm for 30 min at 4°C. $MgCl_2$ was added to the suspension at a concentration of 0.034% and mixed for 10 min at 4°C. Samples were centrifuged at $1000 \times g$ for 5 min at room temperature. The aqueous upper phase was discarded. $MeOH/H_2O/CHCl_3$ (48:47:3) solution was added to the suspension and mixed. Samples were centrifuged at $1000 \times g$ for 5 min at room temperature. The aqueous upper phase was again discarded, and the organic lower phase containing the lipid fraction was transferred to a fresh tube. Collected lipid extracts were desiccated in a vacuum chamber and stored at $-80^\circ C$. Samples were dissolved in $CHCl_3/MeOH$ (2:1) solution before lipidomic analysis.

Mass spectrometry lipidomic analysis

Molecular identification was achieved with high-resolution mass spectrometry using a 9.4 Tesla Solarix XR FT-ICR mass spectrometer (Bruker Daltonics, Billerica, MA) using ramped radio frequency excitation and a 4 MW data set. Lipids were introduced using

syringe flow infusion at a rate of 2 $\mu\text{l}/\text{min}$. Electrospray ionization was performed in both negative and positive ion polarity modes, with continuous accumulation of selected ions used when high mass accuracy for lipid identification was needed. Spectra were analyzed using Data Analysis software (Bruker Daltonics, v. 4.2). Mass spectral peaks were assigned to particular lipids from the LIPID MAPS Lipidomics Gateway (Wellcome Trust) Database using a <2 ppm molecular mass cutoff.

For liquid-extraction surface-analysis mass spectrometry (LESA MS), lipid extracts were spotted on standard glass slides and allowed to dry to completion. LESA was performed on dried spots using a TriVersa nanomate (Advion, Ithaca, NY), and ionization was accomplished with a nanoESI source; the solvent system was 15/35/50 (vol/vol/vol) chloroform:methanol:isopropanol with 7.5 mM ammonium acetate. Sample parameters for LESA: solvent volume was 2.5 μl , dispense volume was 1.7 μl , postdispense delay was 1.0 s, aspiration volume was 2.0 μl , postaspiration delay was 1.0 s, dispensation height was 0.2 mm, aspiration height was 0 mm, delivery gas pressure was 0.3 psi, voltage was 1.4 kV, in both positive and negative modes. Mass spectra were acquired using an amazonSpeed ion trap mass spectrometer with trapControl software (Bruker Daltonics, Billerica, MA). MS acquisition was performed in both negative and positive ion polarity modes. Negative-mode parameters were as follows: end-plate offset (200 V), target ions (70,000), accumulation time (50 ms), mass scan range (m/z 100–1000). Positive mode parameters were as follows: end-plate offset (200 V), target ions (200,000), accumulation time (50 ms), mass scan range (m/z 100–1000). Total injection time was 1 min per sample. Spectra were analyzed using Data Analysis software (Bruker Daltonics, v. 4.2).

Measurement of the generation of palmitoleic acid from palmitic acid

^{13}C -Labeled palmitic acid (605808; Sigma) was dissolved in absolute ethanol and supplemented to logarithmic-phase cells grown in YPD media at a final concentration of 50 μM for 7 h. Cells were extensively washed in sterile water to remove free labeled fatty acids. Cellular lipids were then extracted and the relative abundance of labeled 16:0 and labeled 16:1 was determined by FT-ICR MS as described earlier. The abundance of labeled 16:1 is expressed as a percentage of the total labeled fatty acid to account for any differences in uptake of the labeled 16:0.

Reverse transcription-PCR (RT-PCR)

RT-PCR was performed as previously described (Guerra-Moreno and Hanna, 2016). *OLE1* was amplified with the following primers: 5'-TGAATAACTGGCACCACATTTGAA-3' and 5'-ATCATCAGTCATATCGGTAATATCA-3'. *FAT1* was amplified with the following primers: 5'-CATGCCATTGTTCCATTCAA-3' and GGTCTCAGCCCGTTACCATA-3'. *ACT1* was amplified with the following primers: 5'-CTGGTATGTTCTAGCGCTTG-3' and 5'-GATACCTTGGTGTCTTGGTC-3'. *HAC1* was amplified with the following primers: 5'-CACTCGTCGTCTGATACG-3' and 5'-CATTCAATTCAAATGAATCAAACCTG-3'. These primers flank *HAC1*'s 3'-intron, and thus amplify both the spliced and unspliced forms of *HAC1* mRNA. The UPR was induced by treating cells with tunicamycin (5 $\mu\text{g}/\text{ml}$) for 1 h.

Ole1 depletion

Ole1 depletion was performed by culturing p^{Gal1} -3xHA-*OLE1* strains in YPGal until mid-logarithmic phase. Cultures were washed twice with distilled water and resuspended in YPD medium for the indicated times.

Fluorescence microscopy

Logarithmically growing yeast cultures were concentrated by gentle centrifugation (2 min at 3200 rpm) and resuspended in filter sterilized YPD medium. Confocal microscopy was performed on live cells. mCherry-tagged Htb2 (histone H2B) was used as a nuclear marker.

Images were acquired using an Olympus FV1200 Confocal Microscope equipped with 100 \times oil-immersion objective. Twelve z-stacks of 0.3- μm optical-section spacing were acquired for each image. Images were processed using ImageJ (National Institutes of Health).

ACKNOWLEDGMENTS

We thank Roger Schneider and David Pincus for strains; Erinc Hallacli for assistance with some experiments; and members of the Hanna laboratory for comments on the article. This work was supported by National Institutes of Health grant DP5-OD019800 (to J.H.).

REFERENCES

- Ariyama H, Kono N, Matsuda S, Inoue T, Arai H (2010). Decrease in membrane phospholipid unsaturation induces unfolded protein response. *J Biol Chem* 285, 22027–22035.
- Black PN, DiRusso CC (2007). Yeast acyl-CoA synthetases at the crossroads of fatty acid metabolism and regulation. *Biochim Biophys Acta* 1771, 286–298 [correction published in *Biochim Biophys Acta* (2007). 1771, 911].
- Carman GM, Han GS (2009). Regulation of phospholipid synthesis in yeast. *J Lipid Res* 50, S69–S73.
- Choi JY, Martin CE (1999). The *Saccharomyces cerevisiae* *FAT1* gene encodes an acyl-CoA synthetase that is required for maintenance of very long chain fatty acid levels. *J Biol Chem* 274, 4671–4683.
- Cox JS, Chapman RE, Walter P (1997). The unfolded protein response coordinates the production of endoplasmic reticulum protein and endoplasmic reticulum membrane. *Mol Biol Cell* 8, 1805–1814.
- Cox JS, Walter P (1996). A novel mechanism for regulating activity of a transcription factor that controls the unfolded protein response. *Cell* 87, 391–404.
- De Smet CH, Vittone E, Scherer M, Houweling M, Liebisch G, Brouwers JF, de Kroon AI (2012). The yeast acyltransferase Sct1p regulates fatty acid desaturation by competing with the desaturase Ole1p. *Mol Biol Cell* 23, 1146–1156.
- Ernst R, Ejsing CS, Antonny B (2016). Homeoviscous adaptation and the regulation of membrane lipids. *J Mol Biol* 428, 4776–4791.
- Fu S, Yang L, Li P, Hofmann O, Dicker L, Hide W, Lin X, Watkins SM, Ivanov AR, Hotamisligil GS (2011). Aberrant lipid metabolism disrupts calcium homeostasis causing liver endoplasmic reticulum stress in obesity. *Nature* 473, 528–531.
- Gardarin A, Chédin S, Lagniel G, Aude JC, Godat E, Catty P, Labarre J (2010). Endoplasmic reticulum is a major target of cadmium toxicity in yeast. *Mol Microbiol* 76, 1034–1048.
- Ghaste M, Mistrik R, Shulaev V (2016). Applications of Fourier transform ion cyclotron resonance (FT-ICR) and orbitrap based high resolution mass spectrometry in metabolomics and lipidomics. *Int J Mol Sci* 17, E816.
- Gregor MF, Yang L, Fabbrini E, Mohammed BS, Eagon JC, Hotamisligil GS, Klein S (2009). Endoplasmic reticulum stress is reduced in tissues of obese subjects after weight loss. *Diabetes* 58, 693–700.
- Guerra-Moreno A, Hanna J (2016). Tmc1 is a dynamically regulated effector of the Rpn4 proteotoxic stress response. *J Biol Chem* 291, 14788–14795.
- Halbleib K, Pesek K, Covino R, Hofbauer HF, Wunnicke D, Hänel I, Hummer G, Ernst R (2017). Activation of the unfolded protein response by lipid bilayer stress. *Mol Cell* 67, 673–684.
- Harayama T, Riezman H (2018). Understanding the diversity of membrane lipid composition. *Nat Rev Mol Cell Biol* 19, 281–296.
- Haribowo AG, Hannich JT, Michel AH, Megyeri M, Schuldiner M, Kornmann B, Riezman H (2019). Cytotoxicity of 1-deoxysphingolipid unraveled by genome-wide genetic screens and lipidomics in *Saccharomyces cerevisiae*. *Mol Biol Cell* 30, 2814–2826.
- Hou NS, Gutschmidt A, Choi DY, Pather K, Shi X, Watts JL, Hoppe T, Taubert S (2014). Activation of the endoplasmic reticulum unfolded protein response by lipid disequilibrium without disturbed proteostasis in vivo. *Proc Natl Acad Sci USA* 111, E2271–E2280.
- Jonikas MC, Collins SR, Denic V, Oh E, Quan EM, Schmid V, Weibezahn J, Schwappach B, Walter P, Weissman JS, Schuldiner M (2009).

- Comprehensive characterization of genes required for protein folding in the endoplasmic reticulum. *Science* 323, 1693–1697.
- Kihara A (2012). Very long-chain fatty acids: elongation, physiology and related disorders. *J Biochem* 152, 387–395.
- Klug L, Daum G (2014). Yeast lipid metabolism at a glance. *FEMS Yeast Res* 14, 369–388.
- Knittelfelder OL, Kohlwein SD (2017). Lipid extraction from yeast cells. *Cold Spring Harb Protoc* 2017, doi: 10.1101/pdb.prot085449.
- Kutkowska-Kaźmierczak A, Rydzanicz M, Chlebowski A, Kłosowska-Kosicka K, Mika A, Gruchota J, Jurkiewicz E, Kowalewski C, Pollak A, Stradowska TJ, et al. (2018). Dominant ELOVL1 mutation causes neurological disorder with ichthyotic keratoderma, spasticity, hypomyelination and dysmorphic features. *J Med Genet* 55, 408–414.
- Mueller N, Sassa T, Morales-Gonzalez S, Schneider J, Salchow DJ, Seelow D, Knierim E, Stenzel W, Kihara A, Schuelke M (2019). De novo mutation in *ELOVL1* causes ichthyosis, acanthosis nigricans, hypomyelination, spastic paraplegia, high frequency deafness and optic atrophy. *J Med Genet* 56, 164–175.
- Oh CS, Toke DA, Mandala S, Martin CE (1997). *ELO2* and *ELO3*, homologues of the *Saccharomyces cerevisiae* *ELO1* gene, function in fatty acid elongation and are required for sphingolipid formation. *J Biol Chem* 272, 17376–17384.
- Ozcan U, Cao Q, Yilmaz E, Lee AH, Iwakoshi NN, Ozdelen E, Tuncman G, Görgün C, Glimcher LH, Hotamisligil GS (2004). Endoplasmic reticulum stress links obesity, insulin action, and type 2 diabetes. *Science* 306, 457–461.
- Pineau L, Colas J, Dupont S, Beney L, Fleurat-Lessard P, Berjeaud JM, Bergès T, Ferreira T (2009). Lipid-induced ER stress: synergistic effects of sterols and saturated fatty acids. *Traffic* 10, 673–690.
- Promlek T, Ishiwata-Kimata Y, Shido M, Sakuramoto M, Kohno K, Kimata Y (2011). Membrane aberrancy and unfolded proteins activate the endoplasmic reticulum stress sensor Ire1 in different ways. *Mol Biol Cell* 22, 3520–3532.
- Radanovi T, Reinhard J, Ballweg S, Pesek K, Ernst R (2018). An emerging group of membrane property sensors controls the physical state of organellar membranes to maintain their identity. *Bioessays* 40, e1700250.
- Rutkowski DT, Hegde RS (2010). Regulation of basal cellular physiology by the homeostatic unfolded protein response. *J Cell Biol* 189, 783–794.
- Sinensky M (1971). Temperature control of phospholipid biosynthesis in *Escherichia coli*. *J Bacteriol* 106, 449–455.
- Sinensky M (1974). Homeoviscous adaptation—a homeostatic process that regulates the viscosity of membrane lipids in *Escherichia coli*. *Proc Natl Acad Sci USA* 71, 522–525.
- Singh I, Moser AE, Moser HW, Kishimoto Y (1984). Adrenoleukodystrophy: impaired oxidation of very long chain fatty acids in white blood cells, cultured skin fibroblasts, and amniocytes. *Pediatr Res* 18, 286–290.
- Surma MA, Klose C, Peng D, Shales M, Mrejen C, Stefanko A, Braberg H, Gordon DE, Vorkel D, Ejsing CS, et al. (2013). A lipid E-MAP identifies Ubx2 as a critical regulator of lipid saturation and lipid bilayer stress. *Mol Cell* 51, 519–530.
- Tatzer V, Zellnig G, Kohlwein SD, Schneiter R (2002). Lipid-dependent subcellular relocalization of the acyl chain desaturase in yeast. *Mol Biol Cell* 13, 4429–4442.
- Thibault G, Shui G, Kim W, McAlister GC, Ismail N, Gygi SP, Wenk MR, Ng DT (2012). The membrane stress response buffers lethal effects of lipid disequilibrium by reprogramming the protein homeostasis network. *Mol Cell* 48, 16–27.
- Travers KJ, Patil CK, Wodicka L, Lockhart DJ, Weissman JS, Walter P (2000). Functional and genomic analyses reveal an essential coordination between the unfolded protein response and ER-associated degradation. *Cell* 101, 249–258.
- Vevea JD, Garcia EJ, Chan RB, Zhou B, Schultz M, Di Paolo G, McCaffery JM, Pon LA (2015). Role for lipid droplet biogenesis and microlipophagy in adaptation to lipid imbalance in yeast. *Dev Cell* 35, 584–599.
- Volmer R, van der Ploeg K, Ron D (2013). Membrane lipid saturation activates endoplasmic reticulum unfolded protein response transducers through their transmembrane domains. *Proc Natl Acad Sci USA* 110, 4628–4633.
- Watkins PA, Lu JF, Braiterman LT, Steinberg SJ, Smith KD (2000). Disruption of a yeast very-long-chain acyl-CoA synthetase gene simulates the cellular phenotype of X-linked adrenoleukodystrophy. *Cell Biochem Biophys* 32, 333–337.
- Watkins PA, Lu JF, Steinberg SJ, Gould SJ, Smith KD, Braiterman LT (1998). Disruption of the *Saccharomyces cerevisiae* *FAT1* gene decreases very long-chain fatty acyl-CoA synthetase activity and elevates intracellular very long-chain fatty acid concentrations. *J Biol Chem* 273, 18210–18219.
- Weisshaar N, Welsch H, Guerra-Moreno A, Hanna J (2017). Phospholipase Lpl1 links lipid droplet function with quality control protein degradation. *Mol Biol Cell* 28, 716–725.
- Welch JW, Burlingame AL (1973). Very long-chain fatty acids in yeast. *J Bacteriol* 115, 464–466.
- Wiesinger C, Eichler FS, Berger J (2015). The genetic landscape of X-linked adrenoleukodystrophy: inheritance, mutations, modifier genes, and diagnosis. *Appl Clin Genet* 8, 109–121.